THE JOURNAL OF PHYSICAL CHEMISTRY C

Article

pubs.acs.org/JPCC

Can Starlike C_6Li_6 be Treated as a Potential H_2 Storage Material?

Santanab Giri,[†,‡,§] Fernando Lund,*[,†,‡] Alvaro S. Núñez,[†,‡] and Alejandro Toro-Labbé*[,§]

[†]Departamento de Física and [‡]CIMAT, Facultad de Ciencias Físicas y Matemáticas, Universidad de Chile, Avenida Blanco Encalada 2008, Santiago, Chile

[§]Laboratorio de Química Teórica Computacional (QTC), Facultad de Química, Pontificia Universidad Católica de Chile, Casilla 306, Correo 22, Santiago, Chile

ABSTRACT: The stability and reactivity of planar starlike C_6Li_6 and its hydrogen-adsorbed analogue were analyzed using density functional theory and ab initio molecular dynamics calculations. The ability of the C_6Li_6 system to trap and liberate hydrogen in its molecular form at different temperatures has been established. Interestingly, the planarity of C_6Li_6 is mostly conserved even at high temperature, making this molecule a good candidate to serve as a hydrogen-storage material.

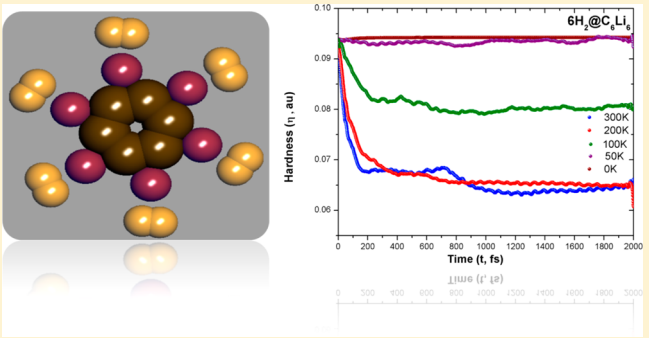

1. INTRODUCTION

The idea to use hydrogen as an alternative fuel was conceived during the past decade and has now became a major research area. The storage of hydrogen and its applicability is challenging because of the lack of proper materials that can act as effective storage devices. Over the past few years, several efforts have been made toward designing novel molecular materials that can act as suitable hydrogen-storage materials under ambient conditions.[1−4] A good hydrogen-storage material should be easily available, low in molecular weight, and capable of adsorbing considerable quantities of hydrogen with a sufficient gravimetric weight percentage, and it should exhibit appropriately rapid adsorption−desorption kinetic behavior. Various metal hydrides,[5] polymers,[6] metal organic frameworks (MOFs),[7] and covalent organic frameworks (COFs),[8] among others. have been explored for this purpose. It has been found that porous MOFs and COFs can adsorb H_2 in molecular form through van der Waals interactions between H_2 and the MOF/COF. The adsorption enthalpies for these systems are in the range of 1.0−1.5 kcal/mol,[9] and high temperatures are required for adsorption.

It has also been found that pure carbon interacts very weakly with N_2[10] and H_2.[11] The adsorption can be improved by adding a charged species because the very poor van der Waals surface is not capable of trapping H_2. Zhao et al.[12] and Yildrim and Ciraci[13] reported that transition-metal-doped fullerene and single-walled carbon nanotubes can efficiently bind H_2. The potential abilities of a variety of molecular motifs, including carbon-based nanomaterials,[14−17] transition-metal-doped boron nitride (BN) systems,[18] aluminum nitride (AlN) nanostructures,[19] fullerene clusters,[20] alkali-metal-doped benzenoid systems,[21] boron−lithium clusters,[22] boron bucky balls (B_{80}),[23] magnesium clusters,[24] and metal−organic frameworks (MOFs),[25] to serve as effective hydrogen-storage materials have been modeled both experimentally and theoretically.

The research group of Chattaraj has shown that aromatic all-metal Li_3^+ and Na_3^+ systems,[26] as well as alkaline-earth-metal cages (M_n, where M = Mg, Ca; n = 8−10),[26] clathrate hydrate molecules,[27] Li-bound neutral and cationic B_n complexes,[28] transition-metal−ethylene complexes[29], and cagelike $B_{12}N_{12}$ clusters[30], can be conceived as prospective materials for the trapping and storage of hydrogen in both atomic and molecular forms. Recently, Giri et al. showed[31] that a carbon−lithium-based molecule, C_6Li_6 can trap 6−12 H_2 molecules in molecular form with a good gravimetric weight percentage (9.6 wt % for $6H_2@C_6Li_6$), thus indicating the promising nature of this potential storage material. Six Li atoms bind with benzene in such a way that they can form star-shaped structures. In fact, it was already established that Li prefers the bridging position of a C−C bond rather than binding directly to a carbon atom.[32−34] It was found that, although starlike C_6Li_6 is not the global minimum-energy structure for this system, it is a true minimum on the potential energy surface. Several studies have been conducted on this system to obtain its stability information.[31,35] In this work, an attempt has been made to determine whether the starlike C_6Li_6 system is truly stable upon variation of the temperature and whether it can be treated as an efficient hydrogen-storage material in terms of rapid adsorption−desorption kinetic behavior.

Received: September 26, 2012
Revised: January 8, 2013
Published: January 9, 2013

2. COMPUTATIONAL DETAILS

For the optimization of starlike C_6Li_6 and its hydrogen-adsorbed analogue $6H_2@C_6Li_6$, we used the B3LYP[36] and M052X[37] functionals with the 6-311+G(d,p) and 6-311G(d) basis sets. The results that we obtained with this approach were consistent with those published previously by Giri et al.[31] After obtaining the optimized geometries, we performed ab initio molecular dynamics (MD) simulations[38] based on atom density matrix propagation (ADMP)[39] to determine whether the two structures are truly stable. ADMP is an extended Lagrangian approach to molecular dynamics using Gaussian basis functions and propagating the density matrix along the classical nuclear degrees of freedom. The ADMP method has been found to be quite interesting, because it provides about the same information as Born−Oppenheimer MD at less computational cost. The B3LYP/6-311G(d) level of theory was used in ADMP calculations.

For C_6Li_6, we performed four different simulations at four different temperatures (0−300 K). Five different trajectories at five different temperatures were generated for $6H_2@C_6Li_6$. For all cases, a thermostat was employed to maintain the temperature constant throughout the simulation. Trajectories of 2 ps were generated for all simulations with a 1-fs time interval. The initial value for the nuclear kinetic energy was set according to a Boltzmann distribution. A default fictitious electron mass (0.1 amu) was chosen for all simulation. To generate the initial Cartesian velocities, a default random number generator seed was used. We performed the dynamics with converged self-consistent-field (SCF) results at each point. At each point of the simulation, it was possible to obtain the structural and frontier-molecular-orbital [highest occupied molecular orbital (HOMO) and lowest unoccupied molecular orbital (LUMO)] energy information. Different conceptual[40] density-functional-theory- (DFT-) based reactivity descriptors such as the chemical potential,[41] hardness,[42] and electrophilicity,[43] were calculated using the HOMO and LUMO energies. All optimization and dynamics runs were performed using the Gaussian 09W suite of programs.[44]

3. RESULTS AND DISCUSSION

In this work, an attempt was made to determine the stability and reactivity of C_6Li_6 and its hydrogen-adsorbed analogue using ab initio molecular dynamics, specifically, the ADMP method. The chemical potential, hardness, and electrophilicity values of these systems are reported in Table 1. Koopmans' theorem[45] was used to calculate these reactivity descriptors. We found that there was not much difference in the values of these descriptors between the 6-311+G(d,p) and 6-311G(d) basis sets. The trends of these descriptors are also consistent with the previously published results of the Chattaraj group,[26−31] although they used the ΔSCF method in their calculations. Figure 1 presents the optimized geometries of C_6Li_6 and $6H_2@C_6Li_6$. For hydrogen-adsorbed C_6Li_6, we found no direct bond between Li and molecular H_2, although this structure is still stable because of a possible ion−induced-dipole interaction between positively charged Li and H_2. It was reported earlier that positively charged Li is capable of trapping H_2 in its molecular form. The positively charged Li could induce a dipole moment in the approaching H_2 molecule, thus creating a possible ion−induced-dipole interaction to stabilize the system.[21,27,46] We also found that, in C_6Li_6, all of the Li atoms are positively charged and the charge on Li decreases when C_6Li_6 binds with molecular H_2 in $6H_2@C_6Li_6$. We also found that the H−H distance increases when hydrogen is trapped on Li.

Table 1. Chemical Potential (μ), Hardness (η), and Electrophilicity (ω) Values of the C_6Li_6 and $6H_2@C_6Li_6$ Systems Obtained Using Koopmans' Theory at the B3LYP Level of Theory[a,b]

system	μ (eV)	η (eV)	ω (eV)
H_2	−5.123/−5.143	13.370/13.494	0.979/0.980
C_6Li_6	−2.119/ −2.113	1.899/1.900 (4.118)	1.182/1.174 (0.715)
$6H_2@C_6Li_6$	1.798/1.760	2.504/2.565 (4.434)	0.646/0.604 (0.518)

[a]Values reported for the 6-311+G(d,p)/6-311G(d) basis sets. [b]Values in parentheses calculated in ref 31 by the ΔSCF method.

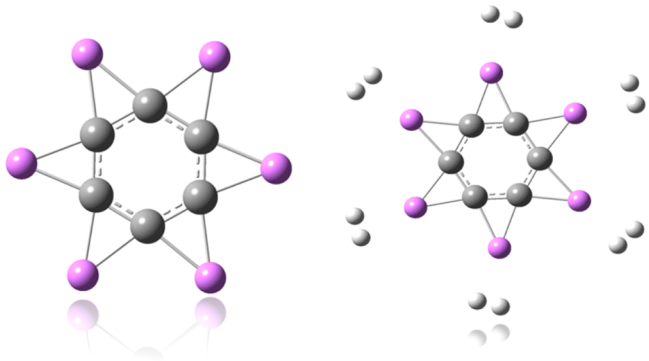

Figure 1. Optimized geometries of the C_6Li_6 and $6H_2@C_6Li_6$ systems at the B3LYP/6-311G(d) level of theory.

To investigate the stability of C_6Li_6, we performed ab initio MD simulations using the optimized geometry obtained from Gaussian 09. Four different 2-ps trajectories at four different temperatures were generated for this purpose. The corresponding potential energy trajectories along with their 2-ps structures are presented in Figure 2. From Figure 2, it is evident that, as the temperature increased, the energy of the system also increased, as a result of the increase in the nuclear kinetic

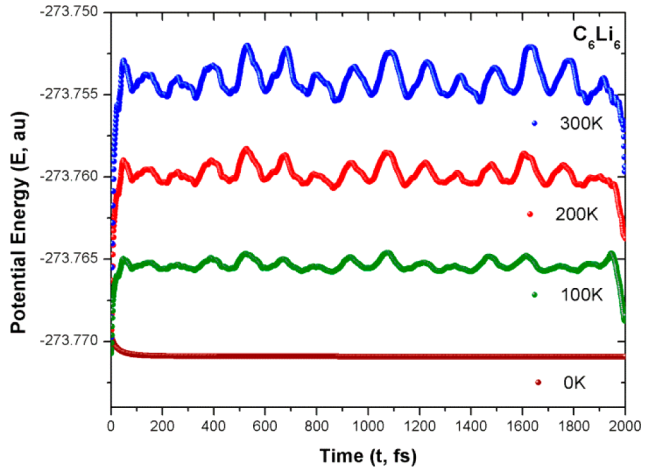

Figure 2. Potential energy trajectories at different temperatures for the C_6Li_6 system. The structures correspond to the 2-ps structures at the respective temperatures.

dx.doi.org/10.1021/jp3095819 | J. Phys. Chem. C 2013, 117, 5544−5551

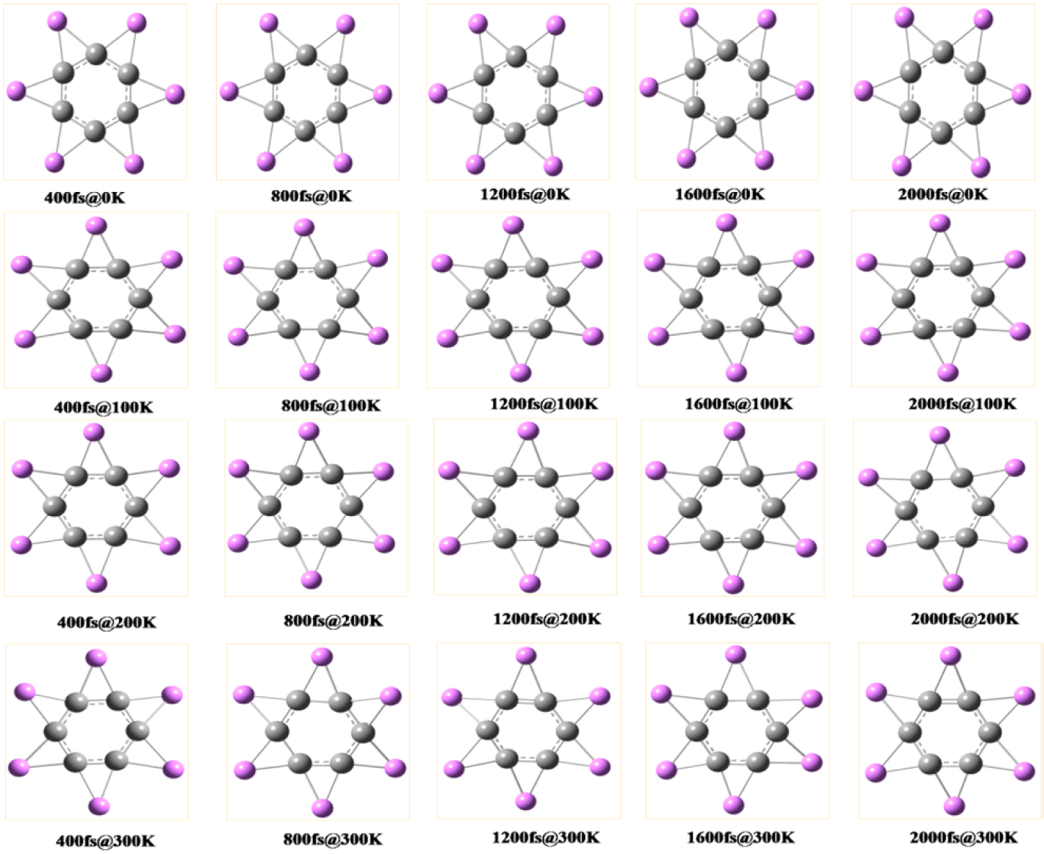

Figure 3. Structures of C_6Li_6 at different time intervals during simulations at different temperatures.

energy. Although it might be expected that the increase in nuclear energy could distort the planarity of C_6Li_6, we found that the planarity of the system was not much affected by a change in temperature. At 0 K, the systems were perfectly planar. As the temperature increased from 100 to 300 K, the geometry became slightly distorted, but this distortion was mainly due to the displacement of Li. Even at room temperature, the planarity of the benzene was not distorted. This is clear when one examines the snapshots of C_6Li_6 taken at different time intervals at different temperatures, as depicted in Figure 3. From these simulations, we concluded that the C_6Li_6 molecule is stable even at room temperature.

Next, we wanted to investigate the stability of $6H_2@C_6Li_6$ and also check whether C_6Li_6 can be treated as a potential hydrogen-storage material. For this purpose, we performed ADMP simulations on the optimized geometry of $6H_2@C_6Li_6$ at various temperatures. Again, a 2-ps trajectory was generated for the simulations at all five temperatures investigated (0, 50, 100, 200, and 300 K). The corresponding potential energies as functions of time are presented in Figure 4. In this case, we again observed that the energy of the system increased with increasing temperature. The stability of this system can be better understood by examining the different snapshots (Figures 5−7) taken during the 2-ps simulations.

At 0 and 50 K, all hydrogen molecules remained trapped on Li in their molecular form. This situation changed when the temperature was increased. At 100 K (Figure 5), we found that, at around 100 fs, one H_2 tried to separate from Li. At 600 fs, another H_2 detached from Li. From that point until the end of the simulation, only two H_2 molecules desorbed from the main structure, leaving four H_2 molecules trapped on Li. As the

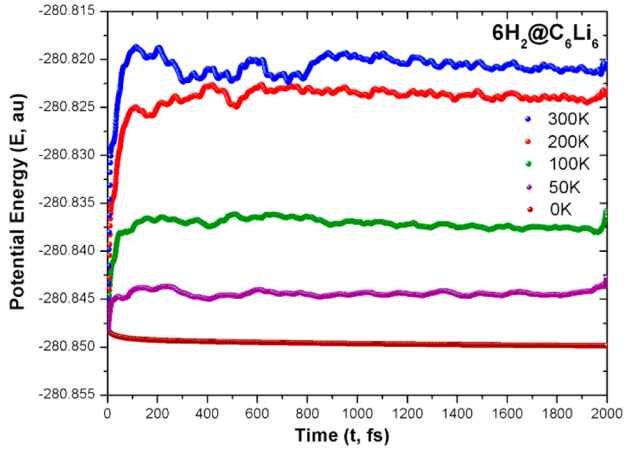

Figure 4. Potential energy trajectories at different temperatures for the $6H_2@C_6Li_6$ system. The structures correspond to the 2-ps structures at the respective temperatures.

temperature increased, the H_2 desorption occurred more quickly. At 200 K, within 200 fs, three H_2 molecules desorbed from Li, and by around 400 fs, four H_2 molecules were completely desorbed from the C_6Li_6 moiety. At the end of the simulation, we found that, at 200 K, all of the H_2 molecules had desorbed and the planar C_6Li_6 was recovered (Figure 6). The same thing happened in the case of the 300 K simulation (Figure 7). In fact, we observed that, at 300 K, H_2 desorption occurred faster than at 200 K. Here, one important point to notice is that the increase in temperature only desorbed the molecular H_2, whereas the parent structure of C_6Li_6 remained

dx.doi.org/10.1021/jp3095819 | J. Phys. Chem. C 2013, 117, 5544−5551

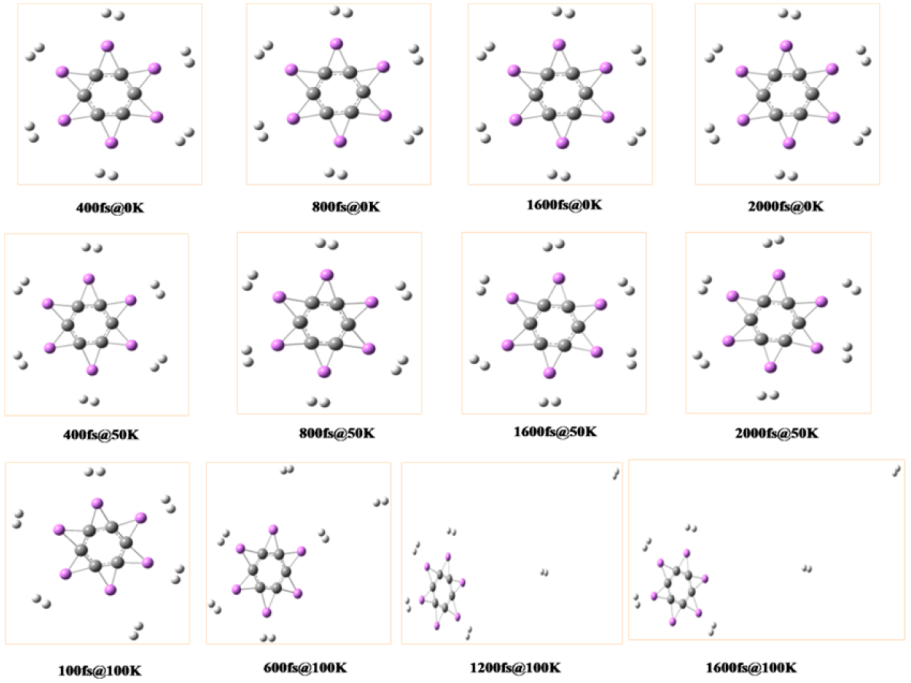

Figure 5. Structures on the potential energy trajectories at different temperatures for the $6H_2@C_6Li_6$ system. The structures correspond to the indicated elapsed times during the 2-ps simulations at the respective temperatures.

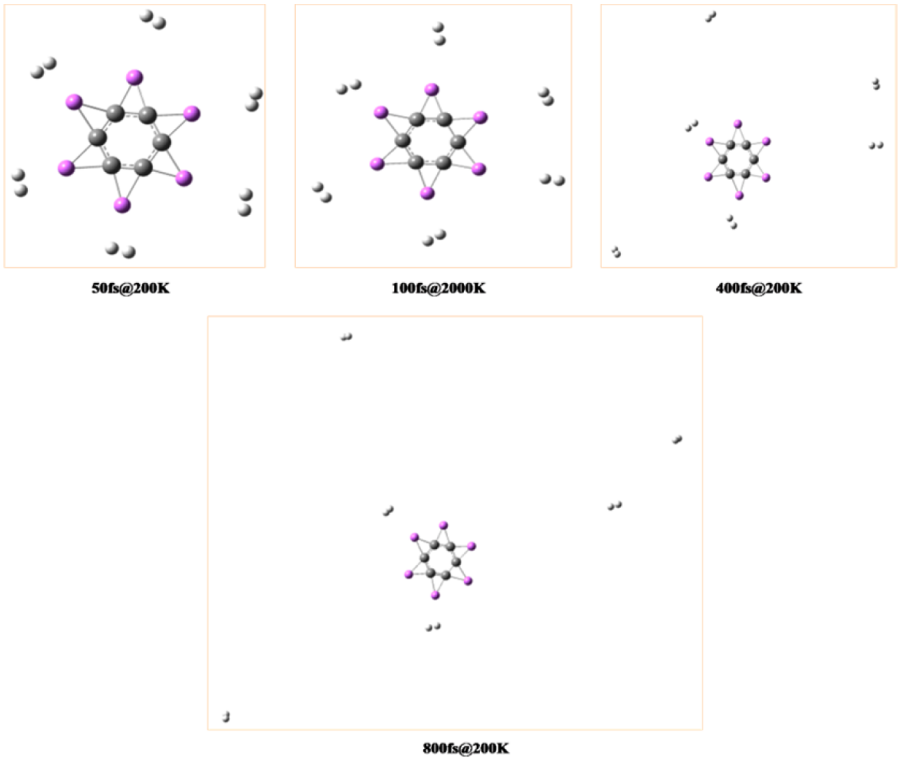

Figure 6. Structures on the potential energy trajectory at 200 K for the $6H_2@C_6Li_6$ system. The structures correspond to the indicated elapsed times during the 2-ps simulation at the given temperature.

unaffected. This fact can also be visualized by examining the potential energy trajectories at 200 and 300 K. The initial oscillation in the potential energy is due to desorption of H_2, but after 800 fs, the trajectories attained a flat region, confirming the complete desorption of all of the H_2 moecules from the C_6Li_6 moiety. Thus, from these simulations, we conclude that C_6Li_6 can be treated as a potential H_2-storage material because it can trap six H_2 molecules at low temperatures and liberate them at higher temperatures. Given that, at high temperature, C_6Li_6 liberates all of the adsorbed H_2 and the parent C_6Li_6 moiety is restored, it is expected that the reactivity of C_6Li_6 can be completely recovered.

To obtain more information about this reactivity pattern, we calculated the conceptual DFT-based global reactivity descrip-

dx.doi.org/10.1021/jp3095819 | J. Phys. Chem. C 2013, 117, 5544−5551

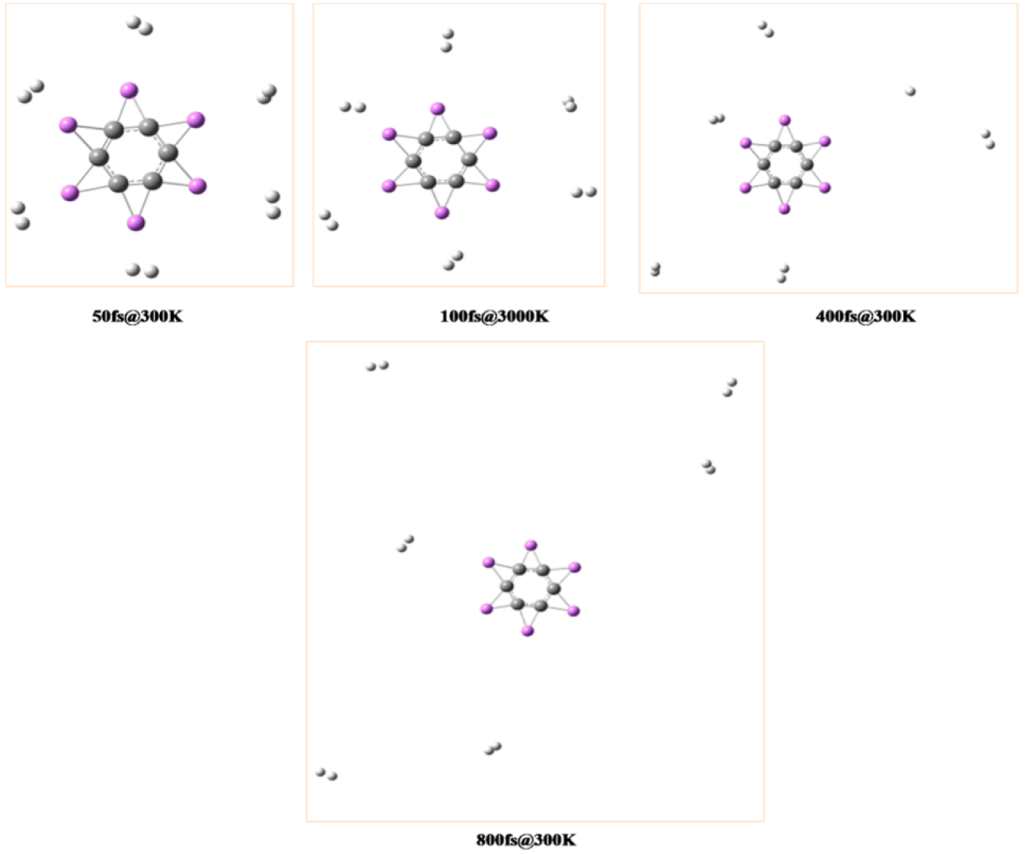

Figure 7. Structures on the potential energy trajectory at 300 K for the $6H_2@C_6Li_6$ system. The structures correspond to the indicated elapsed times during the 2-ps simulation at the given temperature.

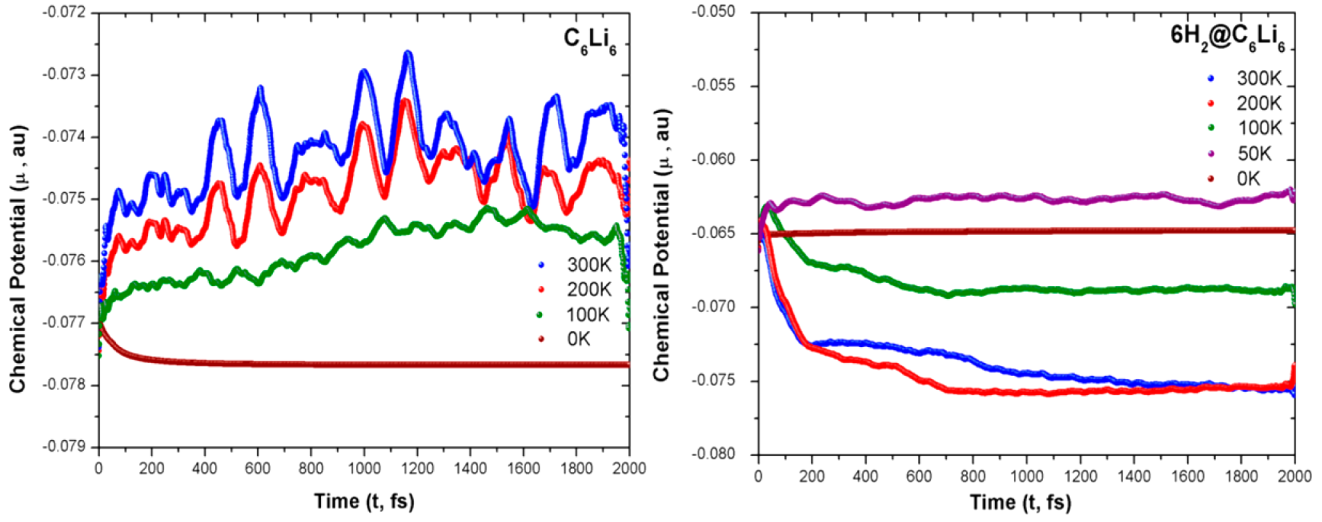

Figure 8. Variations of the chemical potential along the 2-ps simulation for C_6Li_6 and $6H_2@C_6Li_6$ at different temperatures.

tors of chemical potential, hardness, and electrophilicity throughout the simulations. The chemical potential profiles of both C_6Li_6 and $6H_2@C_6Li_6$ are presented in Figure 8. For C_6Li_6, we found that the chemical potential increased with increasing temperature. At 0 and 100 K, it remained constant throughout the simulation. Instantaneous oscillations at higher temperatures such as 200 and 300 K suggest that the chemical potential changes because of the instantaneous change in the external potential. For $6H_2@C_6Li_6$, the pattern was different from that for C_6Li_6. In this case, the chemical potential decreased with increasing temperature except for 50 K. At this temperature, the chemical potential increased from its value at 0 K. From the chemical potential profiles of $6H_2@C_6Li_6$, we observed that, after 1.2 ps, the chemical potentials at 200 and 300 K were almost same, and more interestingly, they attained the value for the parent C_6Li_6 at the respective temperature. This is because, after 1.2 ps, all of the H_2 molecules had desorbed from C_6Li_6, and the planar C_6Li_6 moiety was restored. These results also confirm that the C_6Li_6 moiety is truly stable and can act as a hydrogen-storage material.

dx.doi.org/10.1021/jp3095819 | J. Phys. Chem. C 2013, 117, 5544−5551

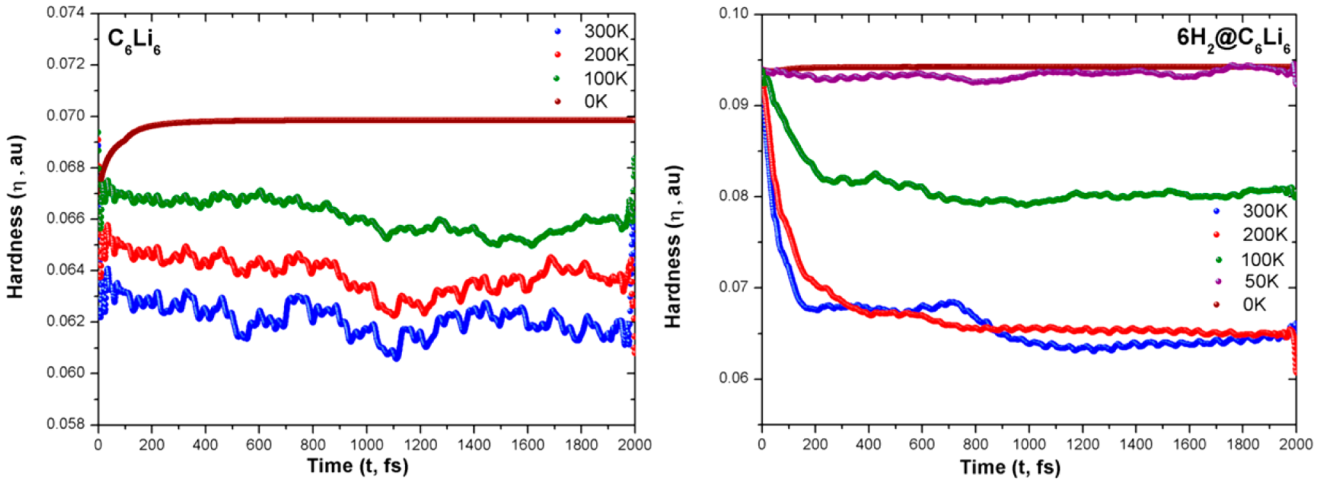

Figure 9. Variations of the hardness along the 2-ps simulation for C_6Li_6 and $6H_2@C_6Li_6$ at different temperatures.

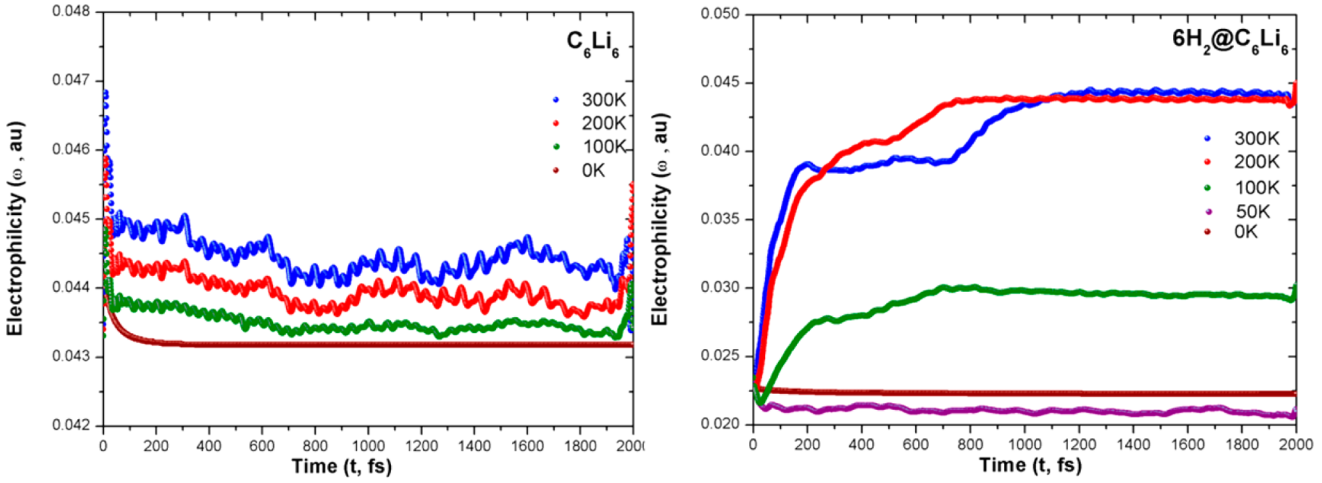

Figure 10. Variations of the electrophilicity along the 2-ps simulation for C_6Li_6 and $6H_2@C_6Li_6$ at different temperatures.

The hardness and electrophilicity profiles of both systems are presented in Figures 9 and 10, respectively. From the plots of hardness, it is evident that hardness decreased with increasing temperature. At 0 and 50 K, the hardness values of the $6H_2@C_6Li_6$ system were almost constant throughout the simulation, indicating that, at these temperatures, $6H_2@C_6Li_6$ is stable. As temperature increased, the stability of $6H_2@C_6Li_6$ decreased because of the structural changes resulting from the desorption of hydrogen from the C_6Li_6 moiety. Here, as for the chemical potential, we found that the hardness values for 200 and 300 K were almost equal to each other after 1.2 ps and equivalent to the value of the parent C_6Li_6 compound.

Electrophilicity increased with increasing temperature, as expected, except at 50 K. At this temperature, we found that the electrophilicity of $6H_2@C_6Li_6$ was less than that for the 0 K profile throughout the simulation time. This indicates that $6H_2@C_6Li_6$ in more stable at 50 than 0 K. For the 200 and 300 K simulations, after 1.2 ps, $6H_2@C_6Li_6$ attained the electrophilicity value of the parent C_6Li_6 moiety at the respective temperatures.

If one examines the hardness and electrophilicity profiles for $6H_2@C_6Li_6$ at high temperature, one can see that the hardness decreased and the electrophilicity increased. This is due to the liberation of H_2 from the C_6Li_6 moiety, which makes the $6H_2@C_6Li_6$ system gradually more reactive. This suggests that $6H_2@C_6Li_6$ is more stable than C_6Li_6, which is also reflected in Table 1. If one considers the reaction between C_6Li_6 and $6H_2$ to produce $6H_2@C_6Li_6$, then, according to the maximum hardness principle (MHP)[47] and the minimum electrophilicity principle (MEP),[48] $6H_2@C_6Li_6$ should be more stable (higher hardness) and less reactive (lower electrophilicity). Exactly this occurred in the present case. From this study, it is now clear that, after all of the hydrogen molecules have been liberated, the $6H_2@C_6Li_6$ complex converts into planar C_6Li_6 + $6H_2$ and all of the reactivity is recovered. In summary, C_6Li_6 is a stable planar compound that can absorb $6H_2$ in its molecular form at very low temperatures and desorb all of the hydrogen molecules at room temperature. Once the H_2 is completely liberated, the C_6Li_6 system is ready to restart the absorption/desorption process again.

4. CONCLUSIONS

The stability and reactivity of C_6Li_6 and $6H_2@C_6Li_6$ were analyzed in terms of energy and conceptual DFT-based reactivity descriptors. All of the analyses revealed that the starlike C_6Li_6 molecule is a very stable compound and its planarity remains conserved even at high temperature. C_6Li_6 can efficiently absorb hydrogen in its molecular form at low temperature and desorb it at room temperature. At high temperature, C_6Li_6 regains it reactivity in terms of chemical

dx.doi.org/10.1021/jp3095819 | J. Phys. Chem. C 2013, 117, 5544−5551

potential, hardness, and electrophilicity after liberating all of the absorbed hydrogen. Therefore, in terms of potential hydrogen-storage materials, C_6Li_6 seems to be a worthy candidate.

AUTHOR INFORMATION

Corresponding Author

*E-mail: atola@puc.cl (A.T.-L.), flund@cimat.cl (F.L.).

Notes

The authors declare no competing financial interest.

ACKNOWLEDGMENTS

The authors thank the Center for Advanced Interdisciplinary Research in Materials (CIMAT) for financial support and the Center for Mathematical Modelling (CMM), Universidad de Chile. This research was partially supported by the supercomputing infrastructure of the NLHPC (ECM-02). S.G. thanks Laboratorio de Química Teórica Computacional (QTC). A.T.-L. gratefully acknowledges funding from FONDECYT through Project 1090460.

REFERENCES

(1) Coontz, R.; Hanson, B. *Science* **2004**, *305*, 957.
(2) Crabtree, G. W.; Dresselhaus, M. S.; Buchanan, M. V. *Phys. Today* **2004**, *57*, 39−56.
(3) Zuttel, A. *Mater. Today* **2003**, *6*, 24−33.
(4) Lubitz, W.; Tumas, W. *Chem. Rev.* **2007**, *107*, 3900−3903.
(5) (a) Schüth, F. *Nature* **2005**, *434*, 712−713. (b) Orimo, S.; Nakamori, Y.; Eliseo, J. R.; Züttel, A.; Jensen, C. M. *Chem. Rev.* **2007**, *107*, 4111−4132.
(6) McKeown, N. B.; Gahnem, B.; Msayib, K. J.; Budd, P. M.; Tattershall, C. E.; Mahmood, K.; Tan, S.; Book, D.; Langmi, H. W.; Walton, A. *Angew. Chem., Int. Ed.* **2006**, *45*, 1804−1807.
(7) Dinca, M.; Daily, A.; Liu, Y.; Brown, C. M.; Neumann, D. A.; Long, J. R. *J. Am. Chem. Soc.* **2006**, *128*, 16876−16883.
(8) Côté, A. P.; Benin, A. I.; Ockwig, N. W.; O'Keeffe, M.; Matzger, A. J.; Yaghi, O. M. *Science* **2005**, *310*, 1166−1170.
(9) (a) Rowsel, J. L. C.; Millward, A. R.; Park, K. S.; Yaghi, O. M. *J. Am. Chem. Soc.* **2004**, *126*, 5666−5667. (b) Sillar, K.; Hofmann, A.; Sauer, J. *J. Am. Chem. Soc.* **2009**, *131*, 4143−4150. (c) Han, S. S.; Furukawa, H.; Yaghi, O. M.; Goddard, W. A., III. *J. Am. Chem. Soc.* **2008**, *130*, 11580−11581. (d) Frost, H.; Snurr, R. Q. *J. Phys. Chem. C* **2007**, *111*, 18794−18803. (e) Klontzas, E.; Tylianakis, E.; Froudakis, G. E. *Nano Lett.* **2010**, *10*, 452−454.
(10) Yang, J.; Sudik, A.; Wolverton, C.; Siegel, D. J. *Chem. Soc. Rev.* **2010**, *39*, 656−675.
(11) Henwood, D.; David Carey, J. *Phys. Rev. B* **2007**, *75*, 245413-1−245413-10.
(12) Zhao, Y.; Kim, Y.-H.; Dillon, A. C.; Heben, J. M.; Zhang, S. B. *Phys. Rev. Lett.* **2005**, *94*, 155504-1−155504-4.
(13) Yildirim, T.; Ciraci, S. *Phys. Rev. Lett.* **2005**, *94*, 175501-1−175501-4.
(14) (a) Xu, W.-C.; Takahashi, K.; Matsuo, Y.; Hattori, Y.; Kumagai, M.; Ishiyama, S.; Kaneko, K.; Iijima, S. *Int. J. Hydrogen Energy* **2007**, *32*, 2504−2512. (b) Strobel, R.; Garche, J.; Moseley, P. T.; Jorissen, L.; Wolf, G. *J. Power Sources* **2006**, *159*, 781−801.
(15) Lochan, R. C.; Head-Gordon, M. *Phys. Chem. Chem. Phys.* **2006**, *8*, 1357−1370.
(16) Ding, R. G.; Finnerty, J. J.; Zhu, Z. H.; Yan, Z. F.; Lu, G. Q. In *Encyclopedia of Nanoscience and Nanotechnology*; Nalwa, H. S., Ed.; American Scientific Publishers: Valencia, CA, 2004; Vol. *X*, pp 1−21.
(17) (a) Dresselhaus, M. S.; Williams, K. A.; Eklund, P. C. *MRS Bull.* **1999**, *24*, 45−50. (b) Froudakis, G. E. *J. Phys.: Condens. Matter* **2002**, *14*, R452−R465.
(18) Shevlina, S. A.; Guo, Z. X. *Appl. Phys. Lett.* **2006**, *89*, 153104-1−153104-3.
(19) Wang, Q.; Sun, Q.; Jena, P.; Kawazoe, Y. *ACS Nano* **2009**, *3*, 621−626.
(20) Peng, Q.; Chen, G.; Mizuseki, H.; Kawazoe, Y. *J. Chem. Phys.* **2009**, *131*, 214505-1−214505-8.
(21) Srinivasu, K.; Chandrakumar, K. R. S.; Ghosh, S. K. *Chem. Phys. Chem* **2009**, *10*, 427−435.
(22) (a) Yildirim, E. K.; Guvenc, Z. B. *Int. J. Hydrogen Energy* **2009**, *34*, 4797−4816. (b) Wu, X.; Gao, Y.; Zeng, X. C. *J. Phys. Chem. C* **2008**, *112*, 8458−8463.
(23) Wu, G.; Wang, J.; Zhang, X.; Zhu, L. *J. Phys. Chem. C* **2009**, *113*, 7052−7057.
(24) Wagemans, R. W. P.; van Lenthe, J. H.; de Jongh, P. E.; van Dillen, A. J.; de Jong, K. P. *J. Am. Chem. Soc.* **2005**, *127*, 16675−16680.
(25) (a) Rosi, N. L.; Eckert, J.; Eddaoudi, M.; Vodak, D. T.; Kim, J.; O'Keeffe, M.; Yaghi, O. M. *Science* **2003**, *300*, 1127−1129. (b) Dinca, M.; Dailly, A.; Liu, Y.; Brown, C. M.; Neumann, D. A.; Long, J. R. *J. Am. Chem. Soc.* **2006**, *128*, 16876−16883. (c) Peterson, V. K.; Liu, Y.; Brown, C. M.; Kepert, C. J. *J. Am. Chem. Soc.* **2006**, *128*, 15578−15579. (d) Forster, P. M.; Eckert, J.; Heiken, B. D.; Parise, J. B.; Yoon, J. W.; Jhung, S. H.; Chang, J.-S.; Cheetham, A. K. *J. Am. Chem. Soc.* **2006**, *128*, 16846−16850.
(26) Giri, S.; Chakraborty, A.; Chattaraj, P. K. *J. Mol. Model.* **2011**, *17*, 777−784.
(27) Chattaraj, P. K.; Sateesh, B.; Mondal, S. *J. Phys. Chem. A* **2011**, *115*, 187−193.
(28) Sateesh, B.; Chakraborty, A.; Giri, S.; Chattaraj, P. K. *Int. J. Quantum Chem.* **2011**, *112*, 695−702.
(29) Chakraborty, A.; Giri, S.; Chattaraj, P. K. *Struct. Chem.* **2011**, *22*, 823−837.
(30) Giri, S.; Chakraborty, A.; Chattaraj, P. K. *Nano Rev.* **2011**, *2*, 5767.
(31) Giri, S.; Sateesh, B.; Chakraborty, A.; Chattaraj, P. K. *Phys. Chem. Chem. Phys.* **2011**, *13*, 20602−20614.
(32) Minkin, V. I.; Minyaev, R. M.; Starikov, A. G.; Gribanova, T. N. *Russ. J. Org. Chem.* **2005**, *41*, 1289−1295.
(33) Smith, B. J. *Chem. Phys. Lett.* **1993**, *207*, 403−406.
(34) Xie, Y. M.; Schaefer, H. F. *Chem. Phys. Lett.* **1991**, *179*, 563−567.
(35) Gao, J. C. *J. Mol. Struct. (THEOCHEM)* **2010**, *953*, 139−142.
(36) (a) Becke, A. *J. Chem. Phys.* **1993**, *98*, 5648−5652. (b) Lee, C.; Yang, W.; Parr, R. G. *Phys. Rev. B* **1988**, *37*, 785−789.
(37) Zhao, Y.; Schultz, N. E.; Truhlar, D. G. *J. Chem. Theory Comput.* **2006**, *2*, 364−382.
(38) Marx, D.; Hutter, J. In *Procedings of Modern Methods and Algorithms of Quantum Chemistry*; Grotendorst, E., Ed.; John von Neumann Institute for Computing: Julich, Germany, 2000.
(39) (a) Schlegel, H. B.; Millam, J. M.; Iyengar, S. S.; Voth, G. A.; Daniels, A. D.; Scuseria, G. E.; Frisch, M. J. *J. Chem. Phys.* **2001**, *114*, 9758−9763. (b) Iyengar, S. S.; Schlegel, H. B.; Millam, J. M.; Voth, G. A.; Scuseria, G. E.; Frisch, M. J. *J. Chem. Phys.* **2001**, *115*, 10291−10302. (c) Schlegel, H. B.; Iyengar, S. S.; Li, X.; Millam, J. M.; Voth, G. A.; Scuseria, G. E.; Frisch, M. J. *J. Chem. Phys.* **2002**, *117*, 8694−8704.
(40) (a) Parr, R. G.; Yang, W. *Density Functional Theory of Atoms and Molecules*; Oxford University Press: New York, 1997. (b) Geerlings, P.; Proft, F. De; Langenaeker, W. *Chem. Rev.* **2003**, *103*, 1793−1874.
(41) (a) Parr, R. G.; Donnelly, R. A.; Levy, M.; Palke, W. E. *J. Chem. Phys.* **1978**, *68*, 3801−3807. (b) *Electronegativity*; Sen, K. D., Jorgensen, C. K., Eds.; Structure and Bonding Series; Springer: Berlin, 1987; Vol. *66*.
(42) (a) Parr, R. G.; Pearson, R. G. *J. Am. Chem. Soc.* **1983**, *105*, 7512−7516. (b) Pearson, R. G. *Chemical Hardness: Applications from Molecules to Solids*; Wiley-VCH: Weinheim, Germany, 1997.
(43) (a) Parr, R. G.; Szentpaly, L. v.; Liu, S. J. *Am. Chem. Soc* **1999**, *121*, 1922−1924. (b) Chattaraj, P. K.; Sarkar, U.; Roy, D. R. *Chem. Rev.* **2006**, *106*, 2065−2091. (c) Chattaraj, P. K.; Roy, D. R. *Chem. Rev.* **2007**, *107*, PR46−PR74. (d) Chattaraj, P. K.; Giri, S.; Duley, S. *Chem. Rev.* **2011**, *111*, PR43−PR75.
(44) Frisch, M. J.; Trucks, G. W.; Schlegel, H. B.; Scuseria, G. E.; Robb, M. A.; Cheeseman, J. R.; Scalmani, G.; Barone, V.; Mennucci,

B.; Petersson, G. A.; Nakatsuji, H.; Caricato, M.; Li, X.; Hratchian, H. P.; Izmaylov, A. F.; Bloino, J.; Zheng, G.; Sonnenberg, J. L.; Hada, M.; Ehara, M.; Toyota, K.; Fukuda, R.; Hasegawa, J.; Ishida, M.; Nakajima, T.; Honda, Y.; Kitao, O.; Nakai, H.; Vreven, T.; Montgomery, J. A., Jr.; Peralta, J. E.; Ogliaro, F.; Bearpark, M.; Heyd, J. J.; Brothers, E.; Kudin, K. N.; Staroverov, V. N.; Keith, T.; Kobayashi, R.; Normand, J.; Raghavachari, K.; Rendell, A.; Burant, J. C.; Iyengar, S. S.; Tomasi, J.; Cossi, M.; Rega, N.; Millam, J. M.; Klene, M.; Knox, J. E.; Cross, J. B.; Bakken, V.; Adamo, C.; Jaramillo, J.; Gomperts, R.; Stratmann, R. E.; Yazyev, O.; Austin, A. J.; Cammi, R.; Pomelli, C.; Ochterski, J. W.; Martin, R. L.; Morokuma, K.; Zakrzewski, V. G.; Voth, G. A.; Salvador, P.; Dannenberg, J. J.; Dapprich, S.; Daniels, A. D.; Farkas, Ö.; Foresman, J. B.; Ortiz, J. V.; Cioslowski, J.; Fox, D. J. *Gaussian 09*, revision B.01; Gaussian, Inc.: Wallingford, CT, 2010.

(45) Koopmans, T. *Physica* **1993**, *91*, 651.

(46) (a) Srinivasu, K.; Chandrakumar, K. R. S.; Ghosh, S. K *Phys. Chem. Chem. Phys.* **2008**, *10*, 5832−5839. (b) Das, R.; Chattaraj, P. K. *J. Phys. Chem. A* **2012**, *116*, 3259−3266.

(47) (a) Pearson, R. G. *J. Chem. Educ.* **1987**, *64*, 561−567. (b) Chattaraj, P. K.; Liu, G. H.; Parr, R. G. *Chem. Phys. Lett.* **1995**, *237*, 171−176. (c) Parr, R. G.; Chattaraj, P. K. *J. Am. Chem. Soc.* **1991**, *113*, 1854−1855. (d) Ayers, P. W.; Parr, R. G. *J. Am. Chem. Soc.* **2000**, *122*, 2010−2018.

(48) (a) Parthasarathi, R.; Elango, M.; Subramanian, V.; Chattaraj, P. K. *Theor. Chem. Acc.* **2005**, *113*, 257−266. (b) Chamorro, E.; Chattaraj, P. K.; Fuentealba, P. *J. Phys. Chem. A* **2003**, *107*, 7068−7072.